Scientia Iranica, Vol. 11, No. 3, pp 234–247
© Sharif University of Technology, July 2004

SCIENTIA
IRANICA

Analysis and Compensation of Receiver Non-Idealities in Wireless OFDM Transceivers

S. Fouladifard[1] and H. Shafiee[*]

High rate wireless communication systems require the design of low-cost radio transceivers with low power consumption. Various architectures for the down conversion of the radio frequency signal to baseband exist. But, with varying degrees, all radio receivers introduce certain non-ideal characteristics of their own, including DC offset, IQ mismatch, frequency offset and phase noise. In this paper, the impact of such non-ideal receiver effects on the performance of an OFDM wireless communication system are investigated. Techniques for compensation or mitigation of such phenomena are discussed and novel methods are proposed.

INTRODUCTION

In a wireless transceiver, prior to demodulation of the received signal, the Radio Frequency (RF) signal needs to be down-converted to the baseband. Various architectures for this operation exist which include the classical heterodyne, direct conversion, image-reject, low-IF and others [1,2]. Different architectures are usually evaluated based on their characteristics with respect to image rejection, adjacent channel rejection, DC offsets, IQ imbalance, spurs and phase noise, as well as their power consumption for a given technology and their suitability for integration.

Image rejection refers to the removal of a spurious signal centered at twice the difference between the carrier and Intermediate Frequency (IF), when applicable. Adjacent channel rejection refers to the filtering out of the signal components in bands adjacent to that of the signal of interest. IQ imbalance refers to phase and gain mismatches between the In-phase (I) and Quadrature (Q) paths [2,3]. Specifically, phase mismatch occurs when the phase difference between the local oscillator signals for I and Q channels is not exactly 90 degrees. Gain imbalance refers to a gain mismatch in the path of the I and Q signals. Spurs are the undesired frequency components within the bandwidth of the signal of interest. Frequency offset is the difference between the received signal carrier frequencies with the local oscillator frequency. In addition to Doppler effects in the wireless channel, frequency offset could be due to the oscillator steady state frequency error, compared to the desired value. Finally, phase noise is the random component present in the phase of the local oscillator waveform.

In classical heterodyne architecture, the signal is first moved to an intermediate frequency before it is mixed again and shifted to baseband. An image-reject filter is employed, prior to the first conversion, while a second channel select filter is used afterwards [2]. The required trade-off between the characteristics of the two filters usually results in the selection of a relatively high intermediate frequency. This, in turn, leads to the bulky Surface Acoustic Wave (SAW) design for the image-reject filter, which is unsuitable for complete integration of the transceiver. On the other hand, adjacent channel rejection can be done quite effectively in this structure. Spurs, DC offset, as well as IQ imbalance effects, do not present major difficulties, though the use of two mixers could increase phase noise power.

In direct conversion receivers, the RF signal is directly converted to baseband and, hence, there is inherently no image signal present. In addition, such designs potentially lead to compact and low power implementations and offer a seamless path toward integration. Low pass filtering of the continuous quadrature waveforms, as well as possible further filtering in the discrete domain, allows excellent adjacent channel rejection. Such features are especially advantageous

1. *Department of Electrical and Computer Engineering, University of Tehran, P.O. Box 11365-4563, Tehran, I.R. Iran.*
*. *Corresponding Author, Department of Electrical and Computer Engineering, University of Tehran, P.O. Box 11365-4563, Tehran, I.R. Iran.*

for mobile terminals and, thus, have generated a great deal of interest for wireless application. On the other hand, DC offsets, spurs and IQ imbalance are more pronounced in such cases. DC offset, for example, could occur due to self-mixing when the local oscillator signal leaks into the receiver input and comes through, along with the desired RF signal. It could also occur when an interference signal becomes present at the receiver input, as well as at the local oscillator output, due to leakage. IQ mismatch occurs due to difficulty in component matching and maintaining identical signal path distances in the I and Q paths at RF.

In the so-called low-IF architectures, the signal is first mixed to an intermediate frequency and the passband signal is then sampled. The down-conversion to baseband is, subsequently, done in the discrete domain. While this architecture has good properties with regard to adjacent channel rejection, IQ mismatch and DC offsets and offers potentials for system integration, it requires Analog-to-Digital Conversion (ADC) at relatively high sampling rates. Design of high rate A/D converters with satisfactory linearity and noise characteristics is, generally, challenging and power inefficient, which has made the practical implementation of low-IF architectures expensive.

In this paper, the impact of the receiver non-idealities, including IQ imbalance, frequency offset and phase noise, on the performance of Orthogonal Frequency Division Multiplexing (OFDM) communication systems will be investigated. OFDM is an effective and spectrally efficient signaling technique for communication over frequency selective channels. Due to its robustness in fading channels and its effectiveness against narrowband interference, OFDM signaling has emerged as the preferred modulation technique in many wireless communication applications. Specifically, OFDM has been proposed or adopted in Digital Audio Broadcasting (DAB), Terrestrial Digital Video Broadcasting (TDVB) and wireless Local-Area Networks (LAN) [3,4].

Mainly, the direct conversion structure will be considered for its simpler mathematical tractability, though the concepts to be discussed are readily adapted to other receiver architectures. The organization of the rest of this paper is as follows: In the next section, a brief outline of OFDM signaling is given and a generic model for the front-end receiver is presented, which includes the non-idealities considered in this paper. Then, the IQ imbalance issue is investigated and two novel algorithms for countering such effects in OFDM transceivers are presented. Next, the effect of frequency offset is investigated and methods for the estimation of its value are discussed. After that, the joint estimation of frequency offset and IQ imbalance parameters are addressed and then phase noise issue and its impact on the performance of the system are presented. Finally, conclusions are included.

OFDM SIGNALING IN WIRELESS COMMUNICATION

The basic principle behind OFDM is to, first, map the (possibly encoded) bit sequence into data symbols using PSK or QAM modulation methods. The symbols are, then, split into groups of N symbols and each symbol is modulated onto one of N orthogonal sub-carriers. The sub-carriers are equally separated by $\Delta f = 1/T$ Hz, where T is the duration of sub-carrier of waveforms. In practice, only sub-carriers in the range $[-K, K]$, where $N \geq (2K+1)$, may be utilized. The signal $x(t)$ is obtained by adding the $(2K+1)$ sub-carrier modulated waveforms together, such that:

$$x(t) = \frac{1}{N} \sum_{k=-K}^{K} X[k] e^{+j2\pi f_k t}, \tag{1}$$

where $X[k]$ is the kth data symbol and $f_k = k\Delta f$ is the kth sub-carrier frequency. By sampling $x(t)$ at instants $t = nT/N$, one will have:

$$x[n] = x(\frac{nT_s}{N}) = \frac{1}{N} \sum_{k=-K}^{K} X[k] e^{+j2\pi k \frac{n}{N}}, \tag{2}$$

where $0 \leq n \leq N-1$. Equation 2 is equivalent to an inverse discrete Fourier transform of the modulated data symbols $X[k]$ and, therefore, could be implemented using Inverse Fast Fourier Transform (IFFT). A complete OFDM symbol is formed by adding N_g guard samples from the end of each block to the beginning. This helps to counter the effect of Inter-Symbol Interference (ISI), as well as Inter-Channel Interference (ICI) [5]. The length of the guard interval is chosen to be greater than the maximum channel delay spread expected.

The real and imaginary components of the IFFT output are converted to continuous-time waveforms using digital-to-analog converters (DAC's) and, then, are low-pass filtered. The signal, $\widetilde{x}(t)$, is, then, up-converted to the desired carrier frequency, f_c, so that the RF signal becomes:

$$s(t) = \widetilde{x}_i(t)\cos(2\pi f_c t) - \widetilde{x}_q(t)\sin(2\pi f_c t), \tag{3}$$

where $\widetilde{x}_i(t)$ and $\widetilde{x}_q(t)$ are in-phase and quadrature inputs to the up-converter, respectively. $s(t)$ is then amplified, using a Power Amplifier (PA), and transmitted.

At the receiver, quadrature demodulation and low–pass filtering of the received RF signal yields the I and Q signals. The continuous-time I and Q

signals are, then, sampled using a pair of analog-to-digital converters. With the length of the guard interval chosen to be longer than the longest delay spread expected, the linear convolution of the transmit sequence and the channel response become equivalent to circular convolution. In the frequency domain, one, thus, has:

$$Y[k] = X[k]H[k] + N[k], \quad k = -K, ..., K, \tag{4}$$

where $Y[k]$ denotes the received signal at sub-channel k, $H[k]$ is the corresponding channel response and $N[k]$ shows the effect of additive noise. To remove the effect of the channel, samples at each sub-channel are multiplied by a one-tap frequency equalizer. Data symbols and the transmitted bit sequence are recovered after the demodulation of the equalized symbols. In Figures 1 and 2, generic block diagrams of the transmitter and receiver in a wireless OFDM communication system, with direct conversion architecture, are shown.

Figure 3 shows the front-end of an OFDM receiver, which also includes several non-ideal effects, namely, DC offsets, frequency offset, IQ imbalance and phase noise. The DC offsets in the I and Q paths are denoted by c_i and c_q, respectively. The gain and phase parameters of IQ mismatch are shown by ε and θ. $\Delta\omega_c$ represents the frequency offset between the transmitter and receiver and the phase noise parameter is shown by $\phi(t)$.

Note that, although DC offset is a major issue in successful implementation of radio receivers, this topic is not specifically addressed in this paper. This is because, in addition to careful circuit design, there are several ways of reducing or eliminating DC offsets

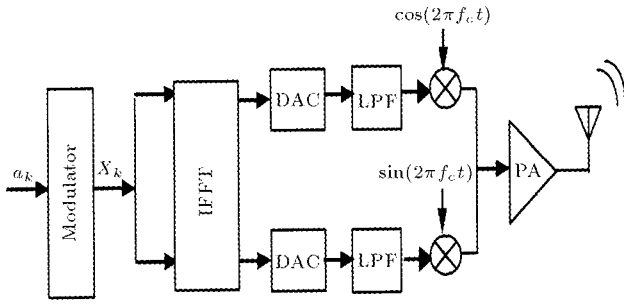

Figure 1. OFDM transmitter.

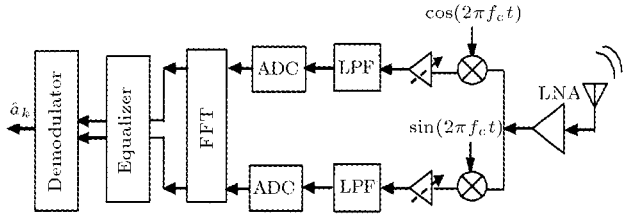

Figure 2. OFDM receiver.

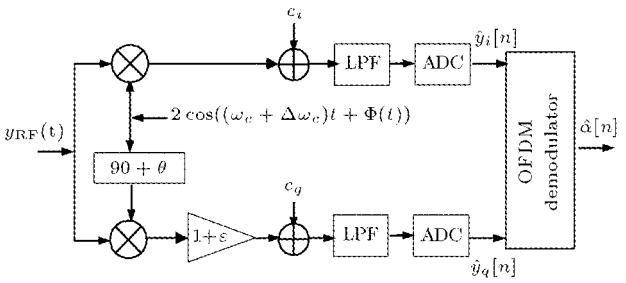

Figure 3. Model of direct converter with non-ideal parameters.

in OFDM communication systems. In the acquisition mode, DC offsets can be removed with the help of analog and digital high-pass filters. The characteristics of these filters may change in the data detection mode. This is done, for example, to prevent the effective overall channel response from being excessively long, which in turn, could overwhelm the available guard interval for each OFDM symbol. In addition, in the design of OFDM symbols, the DC sub-channel is usually filled with zero. This allows the receiver to monitor this value to estimate the residual DC offset and, then, correct the incoming I and Q signals. In the rest of this paper, therefore, the DC offset values, c_i and c_q will be considered equal to zero.

To analyze the impact of the above non-ideal effects on the performance of the system, an OFDM system will be considered whose parameters are set, based on the specifications of IEEE 802.11a standards for Wireless Local Area Networks (WLAN) in the 5 GHz band. Here, the OFDM modulator uses 64 sub-channels, 52 of which are used for data or pilot symbols and the other sub-carriers, which include the DC channel, are filled with zero. Sub-carrier spacing is chosen to be 312.5 kHz, so that the total bandwidth becomes 20 MHz. Computer simulations are performed using the 16-QAM modulation.

IQ IMBALANCE

As mentioned previously, phase imbalance occurs when the phase difference of the local oscillator for the I and Q paths is not exactly 90 degrees, i.e., θ has a non-zero value in Figure 3. Also, gain imbalance occurs when the gain in quadrature paths is not the same, i.e., ε in Figure 3 has a non-zero value. Recently, a few techniques for compensation for IQ imbalance in radio receivers have been proposed [6,7]. In the absence of frequency offset and phase noise, the I and Q signals are related to the ideal down-converted waveforms, $y_i(t)$ and $y_q(t)$, according to the following:

$$\hat{y}_i(t) = y_i(t), \tag{5}$$

$$\hat{y}_q(t) = (1+\varepsilon)\big(y_q(t)\cos(\theta) - y_i(t)\sin(\theta)\big). \tag{6}$$

By taking the discrete Fourier transform of the complex samples, it is readily verified that the sample at the kth sub-carrier in the OFDM receiver will become:

$$\hat{Y}[k] = \gamma Y[k] + \lambda Y^*[-k], \tag{7}$$

where:

$$\gamma = 0.5\Big\{1 + (1+\varepsilon)\big(\cos(\theta) - j\sin(\theta)\big)\Big\}, \tag{8}$$

$$\lambda = 0.5\Big\{1 - (1+\varepsilon)\big(\cos(\theta) + j\sin(\theta)\big)\Big\}. \tag{9}$$

The multiplicative parameters are related such that:

$$\lambda = (1 - \gamma^*). \tag{10}$$

The above relation shows that the gain and phase mismatches in the receiver mixer cause the symbol at the sub-carrier, k, to be multiplied by the complex factor, γ. In addition, a spurious component will be present, which is equal to the conjugate of the symbol at $-k$ sub-carrier, multiplied by another complex term, λ. The sample at the kth sub-carrier, therefore, will include an interference related to the symbol at the $-k$th sub-carrier and vice versa.

Figure 4 shows a plot of symbol error rate (SER) vs SNR per bit (denoted as E_b/N_0) for an Additive White Gaussian Noise (AWGN) channel, with two set of values for mismatch parameters in the receiver. The SER plot for the system, without any IQ imbalance, is also shown for comparison. The plots show that the mismatches degrade the system performance quite severely. Specifically, with ε and θ set at 0.5 dB and 5 degrees, respectively, the SER at an SNR of 14 dB is increased by two orders of magnitude. The degradation is more severe when ε and θ are set at 1.5 dB and 10 degrees, respectively.

In the following sections, two novel techniques are proposed for compensation of the IQ imbalance [8-11]. First, a technique for estimation of the related

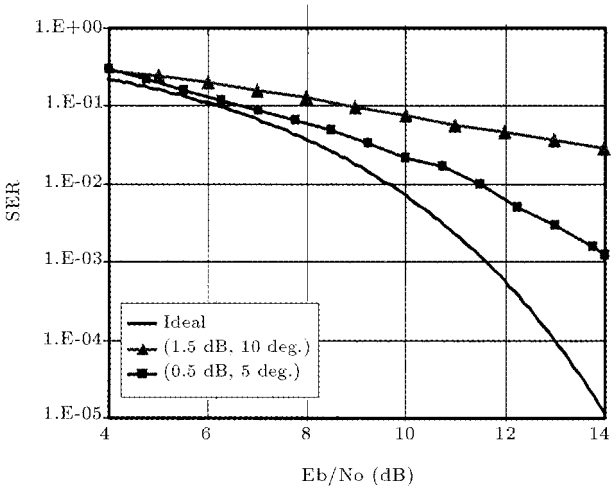

Figure 4. Symbol error rate vs SNR.

parameters and subsequent receiver calibration is discussed. An adaptive method, which compensates for the mismatch in both transmitter and receiver mixers, follows next.

Estimation and Compensation of IQ Mismatch

To measure and compensate for the IQ mismatch in the receiver, the use of specific OFDM symbols, are proposed, such that select sub-carriers $\{k_1, k_2, \cdots, k_r\}$ are nulled, i.e., the symbol allocated to each of these sub-channels is zero. Furthermore, known symbols are placed at their corresponding mirror sub-channels denoted by $\{-k_1, -k_2, \cdots, -k_r\}$. In a calibration mode, or as part of the preamble section, r could be set equal to K, and multiple OFDM symbols, with the above description, can be transmitted. Alternately, one can select a few pilot sub-channels within each OFDM symbol and fill those according to the above configuration, i.e., half of the pilots are filled with a known symbol and the other half, i.e., those whose indices have opposite signs, are filled with zero. Let us suppose that samples at a total of L sub-carriers are collected, which could be part of one or a multiple of OFDM symbols. The set containing the nulled sub-carriers will be donated by S.

The algorithm is based on monitoring the FFT output at sub-carriers, which were filled with zeros. Notice that, based on Equation 7 and in absence of noise, any non-zero values at these bins are due to the gain and phase imbalances. Specifically, at the nulled sub-carrier, k', the received sample will be $\lambda Y^*[-k']$. Next, the estimation problem will be considered in the context of an AWGN channel. The AWGN case can arise in an especially-designed calibration procedure. In this case, the channel frequency response, $H[k]$, will be unity for all sub-carriers. Without loss of generality, let one suppose that the known (non-zero) symbols are set to unity. The received sample at a nulled sub-carrier, k', is given by the following:

$$\hat{Y}[k'] = 0.5\,\{1 - (1-\varepsilon)(\cos(\theta) + j\sin(\theta))\} + \gamma N[k'] + \lambda N^*[-k'], \tag{11}$$

where $N[k']$ and $N[-k']$ denote the zero-mean complex noise samples at sub-carriers k' and $-k'$, respectively. With L samples of data available, an estimate of the phase imbalance is given by the following relation:

$$\hat{\theta} = \tan^{-1}\left(\sum_{k' \in S} \hat{Y}_i[k'] / \Big(\sum_{k' \in S} \hat{Y}_r[k'] - L/2\Big)\right), \tag{12}$$

where $\hat{Y}_r[j]$ and $\hat{Y}_i[k']$ correspond to the real and imaginary components of $\hat{Y}[k']$.

It can be shown that the above estimate is unbiased [8] and the conditional variance of the estimate is given by:

$$Var(\hat{\theta}|\theta) \approx 2(1+(1+\varepsilon)^2)\sigma_i^2/L, \tag{13}$$

where σ_i^2 is the variance of the imaginary component of noise. The above relation shows that the variance of the estimate is decreased, as SNR improves or as L is increased. Therefore, $\hat{\theta}$ is an unbiased and consistent estimate for θ. The value of $\hat{\varepsilon}$ is, subsequently, obtained from the following:

$$\hat{\varepsilon} = -1 + \frac{1}{\cos(\hat{\theta})} - \frac{2}{L\cos(\hat{\theta})} \sum_{k' \in S} \hat{Y}_r[k']. \tag{14}$$

It could be shown that the above estimate has a bias equal to $(1+\varepsilon)\{\cos(\theta)/\cos(\hat{\theta})-1\}$. However, since the estimate of $\hat{\theta}$ is unbiased, the bias in $\hat{\varepsilon}$ will be very small. The conditional variance of $\hat{\varepsilon}$ will be [8]:

$$Var(\hat{\varepsilon}|\varepsilon) = \frac{2}{L\cos^2(\hat{\theta})} \left(1+(1+\varepsilon)^2\right) \sigma_r^2, \tag{15}$$

where σ_r^2 is the variance of the real component of noise. When $\hat{\theta}$ is small, the variance is dominated by the last term, which, again, shows that higher SNR's and larger L's would reduce the variance.

In the case of a frequency selective fading channel and in the absence of noise, the received samples at bins k' and $-k'$ are given as follows:

$$\hat{Y}[k'] = \lambda Y^*[-k'], \tag{16}$$

$$\hat{Y}[-k'] = \gamma Y[-k']. \tag{17}$$

One can, thus, write:

$$\hat{Y}^*[k'] = \beta \hat{Y}[-k'], \tag{18}$$

where:

$$\beta = \lambda^*/\gamma = 1 - \gamma/\gamma. \tag{19}$$

Therefore, estimating the parameter β would result in estimates for γ and λ using Equations 17 and 10, respectively. Consequently, estimates θ and ε are obtained from Equation 8, as given below:

$$\hat{\theta} = -\tan^{-1}(\Im m\{2\hat{\gamma}-1\}/\Re e\{2\hat{\gamma}-1\}), \tag{20}$$

$$\hat{\varepsilon} = -1 + \left(\Re e\{2\hat{\gamma}-1\}/\cos(\hat{\theta})\right). \tag{21}$$

With L nulled sub-carriers available, β is estimated from:

$$\hat{\beta} = \sum_{k' \in S} \hat{Y}^*[k'] / \sum_{k' \in S} \hat{Y}[-k']. \tag{22}$$

If it is again assumed that the contribution due to β is subtracted from each sample of $\hat{Y}[k']$, then, the estimation error is given by:

$$\hat{\beta} - \beta = \frac{|\gamma|^2 - |\lambda|^2}{\gamma \sum\limits_{k' \in S} \hat{y}[-k']} \sum_{k' \in S} N^*[k']. \tag{23}$$

The above relation shows that the estimate will be unbiased, since γ and λ are both deterministic. The variance of the estimate, however, will be data-dependent, which, in turn, will depend on the channel response [8].

When estimates for $\hat{\theta}$ and $\hat{\varepsilon}$ are obtained, the I and Q sequences in the baseband can be processed to cancel the effect of receiver IQ mismatch. The multiplicative parameters are readily obtained from Equation 6. The compensation block is shown in Figure 5, where the parameter g is given by $1/(\cos(\hat{\theta})(1+\hat{\varepsilon}))$.

The above procedure is again tested on an OFDM system designed with IEEE 802.11a parameters. Figures 6 and 7 show the average of the phase and gain mismatch parameters, respectively, obtained using Equations 12 and 14, vs true values for two different values of channel SNR. As expected, the phase estimate is unbiased and the bias of the gain estimate is also negligible. Figures 8 and 9 show the variance of the

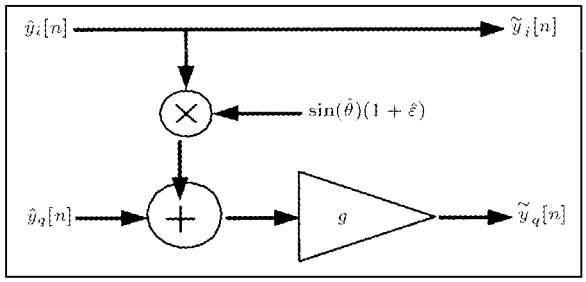

Figure 5. Compensation block.

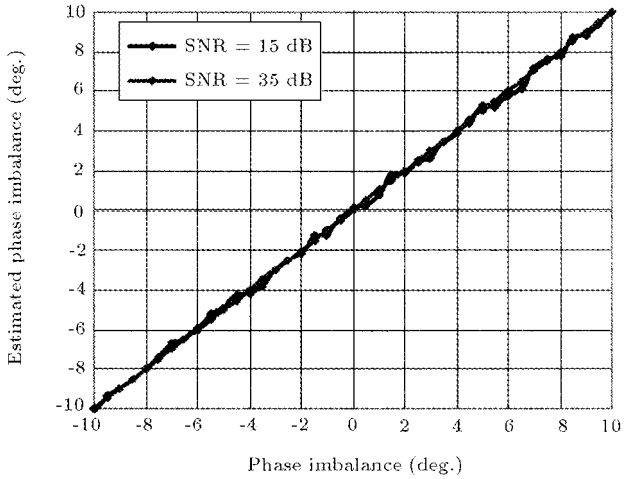

Figure 6. Estimated phase imbalance versus true value (AWGN).

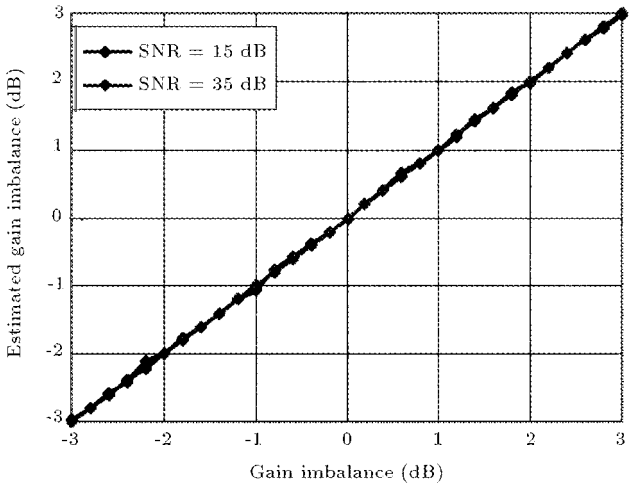

Figure 7. Estimated gain imbalance vs true value (AWGN).

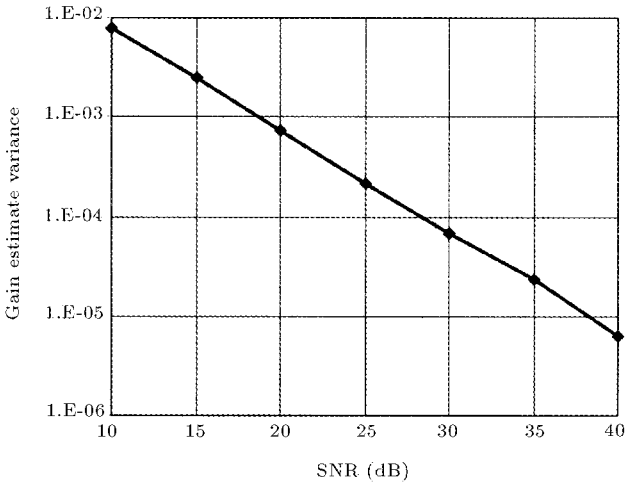

Figure 9. Variance of gain imbalance estimation versus SNR (AWGN).

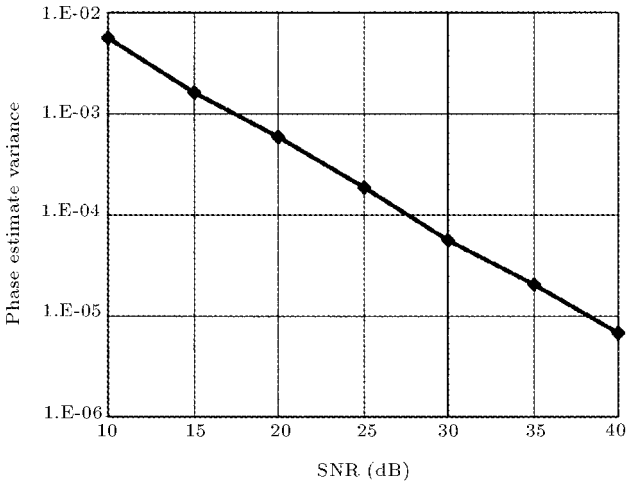

Figure 8. Variance of phase imbalance estimation versus SNR (AWGN).

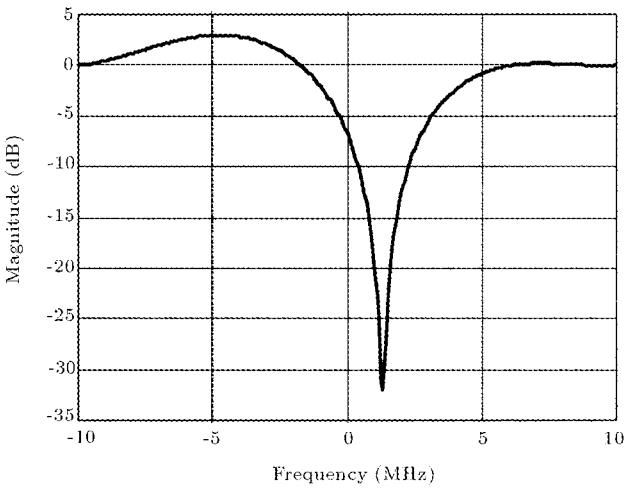

Figure 10. Frequency response of simulated fading channel.

estimates obtained from simulations, which decreases with SNR as predicted by Equations 13 and 15.

Next, to test the estimation algorithm on a frequency selective fading channel, the transmit signal was run through a channel with a fading profile, as shown in Figure 10. Figure 11 shows the average of the phase mismatch parameters, calculated using Equation 20 vs the corresponding true values, shown for two different SNR values. The plot confirms that the proposed estimate is unbiased. The average of the gain parameter obtained using Equation 21 is also plotted vs the true values in Figure 12.

Adaptive Method

IQ imbalance can also be compensated using adaptive techniques. In [12], a frequency domain adaptive algorithm is proposed, which uses a two-tap equalizer for each sub-channel. In this section, an adaptive

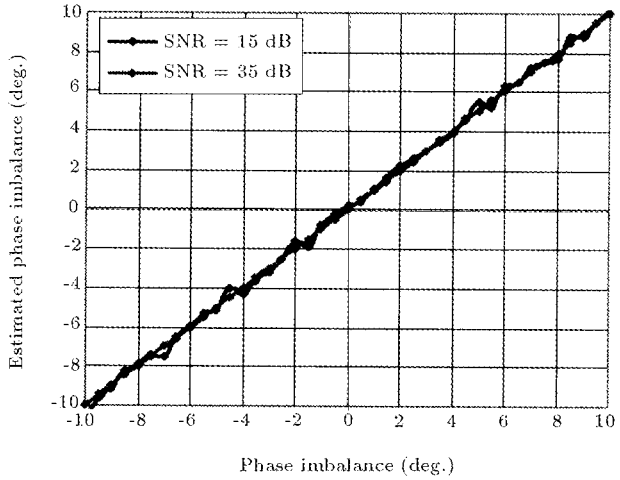

Figure 11. Expected value of the estimated phase mismatch vs the true value (fading channel).

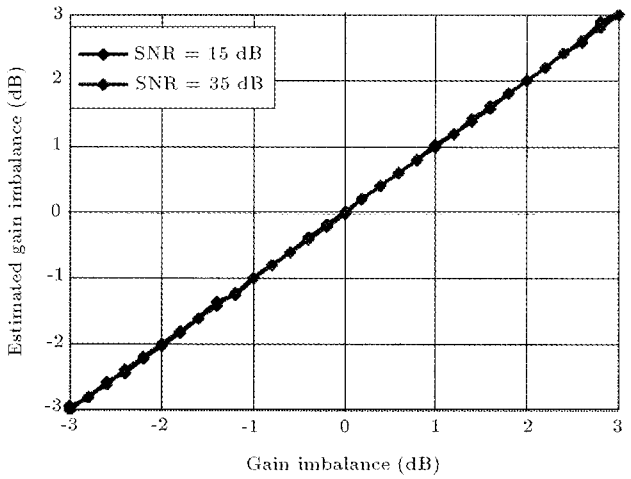

Figure 12. Expected value of the estimated gain mismatch vs the true value (fading channel).

algorithm is proposed, which operates on the time-domain baseband samples [10,11].

The intent is to predict the interference signal in the Q path and subtract it from the incoming signal. A block diagram of the structure of the compensation block is shown in Figure 13.

The mismatch cancellation is undertaken in two stages: First an adaptive filter predicts the interference from the I path and subtracts it from the quadrature signal. Then, the gain in the quadrature path is adjusted, adaptively.

Let one define $y'_q[n]$ as the sample in the quadrature path, after the interference from the in-phase signal is subtracted, i.e.,

$$y'_q[n] = \hat{y}_q[n] - \mathbf{w}^T \hat{\mathbf{y}}_i[n], \tag{24}$$

where $\mathbf{w}$ is the filter coefficient vector and $\hat{\mathbf{y}}_i[n]$ is the vector of input samples, i.e.,

$$\mathbf{w}^T = (w_0, w_1, \cdots, w_{m-1}),$$

$$\hat{\mathbf{y}}_i^T[n] = (\hat{y}_i[n], \hat{y}_i[n-1], \cdots, \hat{y}_i[n-m+1]).$$

From Equation 6, it is evident that the phase imbalance causes each sample of the quadrature signal to be affected by the sample in the in-phase path at the same time interval. With the interference, thus, being memory less, it is sufficient to employ a prediction filter with only one tap. If the expected prediction error power were defined as:

$$J_q = E\left\{\left|y'_q[n]\right|^2\right\}, \tag{25}$$

then, the update equation for the filter coefficient, using the Least Mean Square (LMS) algorithm, would be given by:

$$w(n+1) = w(n) + \mu \hat{y}_i[n].y'_q[n], \tag{26}$$

where μ is the learning constant [8].

Next, the gain parameter is adapted, so that the signal power for the Q path becomes a prescribed fixed value. Let one consider that the target power is given by $(P_s + P_n)$, where P_s is the desired signal power and P_n is the noise power. Also, $e_q[n]$ is defined as the difference between the desired power level and instantaneous power at time n, i.e.,

$$e_q[n] = P_s + P_n - \left|\tilde{y}_q[n]\right|^2. \tag{27}$$

The update equation for the gain parameter to minimize $e_q[n]$ is readily obtained, as given below:

$$g_q[n+1] = g_q[n] + \delta e_q[n], \tag{28}$$

where δ is the step size.

Figure 14 shows the results of applying the above adaptive algorithm when ε and θ, again, were set at 1.5 dB and 10 degrees, respectively. The results were obtained after the adaptive algorithm had converged. The plots show that an adaptive technique cancels non-ideal effects almost entirely.

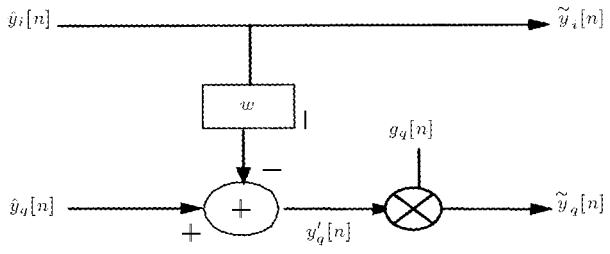

Figure 13. Time domain compensation block.

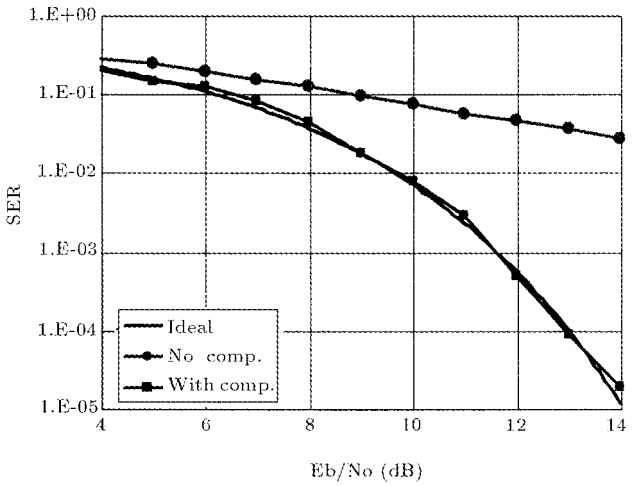

Figure 14. SER performance of compensation algorithms.

FREQUENCY OFFSET

OFDM systems are also quite sensitive to carrier frequency offset, as this also disrupts the orthogonality between sub-carriers. As mentioned in the first section, frequency offset occurs due to a difference in frequencies of the mixers in the transmitter and receiver, or, due to a Doppler shift, due to the relative movement of the modems.

With a frequency offset, $\Delta\omega_c = 2\pi f_c$, the complex envelope of the received sequence will have a multiplicative factor of the form $\exp(j\Delta\omega_c n T_s)$, where n is the sample index and T_s is the sample period. If β denotes the ratio of the frequency offset to the sub-carrier separation, the received samples in one OFDM symbol can be written as:

$$\hat{y}[n] = \frac{1}{N}\sum_{k=-K}^{K} X[k]H[k]e^{j2\pi n\frac{(k+\beta)}{N}} + w_1[n], \qquad (29)$$

where the IQ imbalance and phase noise effects have been ignored. The presence of the factor, $\exp(j2\pi n\beta/N)$, disturbs the orthogonality between sub-carriers and results in Inter-Channel Interference (ICI). It also causes degradation of Signal-to-Noise Ratio (SNR) in each sub-carrier.

The reduction in signal amplitude and the phase rotation of the samples, as well as the effect of ICI caused by the frequency offset, is evident when the OFDM symbol at the output of the FFT block is examined. For the kth sub-channel, one will have [13]:

$$\tilde{Y}[k] = \gamma[k]\frac{\sin(\pi\beta)}{N\sin\left(\frac{\pi\beta}{N}\right)}e^{j\pi\beta\frac{N-1}{N}} + I[k] + W[k], \quad (30)$$

where $Y[k]$ is the signal in absence of frequency offset, $I[k]$ denotes the effect of ICI, which is given by:

$$I[k] = \sum_{\substack{l=-K\\ l\neq k}}^{K} Y[l]\frac{\sin(\pi\beta)}{N\sin(\frac{\pi(l-k+\beta)}{N})}e^{j\pi\beta\frac{N-1}{N}} \times e^{j\pi\frac{l-k}{N}}, \qquad (31)$$

and $W[k]$ shows the effect of additive noise.

To assure effective demodulation of the OFDM signal, the frequency offset has to be removed by adopting a precise matching of the local oscillator frequency to the signal carrier frequency, or else, by correcting the down-converted baseband signal using digital signal processing techniques.

Various techniques have been proposed for the estimation and compensation of frequency offset in OFDM receivers [13,14]. These algorithms, generally, examine the rotation of samples due to frequency offset in time or frequency domains. Specifically, if an OFDM symbol were transmitted twice in a row, each time-domain sample at the receiver would be written as:

$$y'[n] = y[n]e^{j\Delta\omega_c n T_s}, \qquad (32)$$

where $y[n]$ denotes the received sample without any frequency offset. Note that when the amount of the offset is zero, the product, $v[n] = y^*[n]y[n-N]$, is expected to be real. Otherwise, the amount of offset can be estimated from the non-zero phase of $v[n]$, since, in absence of noise, one will have:

$$\Delta\omega_c = \frac{\arg(v[n])}{NT_s}. \qquad (33)$$

Clearly, an unambiguous determination of the value of the frequency offset is undertaken using the above relation, when the offset is in the following range:

$$\frac{-\pi}{NT_s} \leq \Delta\omega_c \leq \frac{\pi}{NT_s}. \qquad (34)$$

Note that for the above procedure to work, the length of the repeated block does not need to be N.

Alternatively, the estimation can be done using frequency domain samples. Again, supposing that an OFDM symbol of length N is transmitted twice in a row, the samples of the second block can be written as:

$$z_2[n] = z_1[n+N] = \frac{1}{N}\sum_{k=-K}^{K} X[k]h(k)e^{j2\pi\frac{(k+\beta)}{N}(n+N)}, \qquad (35)$$

where $0 \leq n \leq N-1$. One can, thus, write:

$$z_2[n] = z_1[n]e^{j2\pi\beta}, \qquad (36)$$

and, in the frequency domain, one will have:

$$Z_2[k] = Z_1[k]e^{j2\pi\beta}. \qquad (37)$$

With noise present, samples in the two consecutive blocks in the frequency domain can, then, be written as:

$$Y_1'[n] = Z_1[k] + N_1[k], \qquad (38)$$

$$Y_2'[k] = Z_1[k]e^{j2\pi\beta} + N_2[k], \qquad (39)$$

where $N_1[k]$ and $N_2[k]$ denote the effect of noise in the kth sub-channel in the first and second block, respectively. Using the above relation, the maximum likely estimate of the frequency offset is given by [13]:

$$\hat{\beta} = \frac{1}{2\pi}\arg\left(\sum_{k=-K}^{K} Y_2'[k]Y_1'^*[k]\right). \qquad (40)$$

It can be shown that the estimate is unbiased and its conditional variance decreases as the channel noise is reduced and the total symbol energy is increased.

In the tracking mode, remnant frequency offset effects are estimated using a similar approach, though here, pilot tones are inserted in each OFDM symbol and the phase rotation of each of these sub-channels is

examined. The remnant offset is found by the following relation [14,15]:

$$\hat{\varepsilon} = \frac{1}{2\pi L} \arg \left\{ \begin{array}{l} \sum_{j=0}^{L_f-1} \left(Y_{(m+L)}(p(j)) Y_m^*(p(j)) \right) \\ \times \left(X_{(m+L)}^*(p(j)) X_m(p(j)) \right) \end{array} \right\}, \quad (41)$$

where m is the OFDM symbol number, L is the number of samples separating symbols containing pilots, L_f is the number of pilots and $p(j)$ is a function, which gives the location of pilots within OFDM symbols. Clearly, instead of using pilots, one can utilize data symbols, along with their corresponding detector output in a decision directed manner.

The above frequency domain algorithm is tested on the IEEE 802.11a OFDM system, described previously. Here, channel SNR is set at a relatively large value. In Figure 15, the mean of the frequency offset estimates, obtained using Equation 40, is plotted vs its corresponding true value, which shows that, as expected, the estimate is unbiased. In this figure, assuming a carrier frequency of 5 GHz, the offset is shown in ppm (parts per million), which means that the range 0 to 24 ppm corresponds to values of β ranging from 0 to 0.39. In Figure 16, the standard deviation of the estimate is plotted, which shows that this value is independent of the value of offset.

JOINT ESTIMATION AND COMPENSATION OF FREQUENCY OFFSET AND IQ IMBALANCE

When the gain and phase mismatch values are not zero in the mixer at the receiver, the relation between phases of the samples of $\tilde{Y}_1[k]$ and $\tilde{Y}_2[k]$, shown in Equations 38 and 39, no longer holds and the frequency estimation algorithms, which attribute all phase differences between like samples to frequency

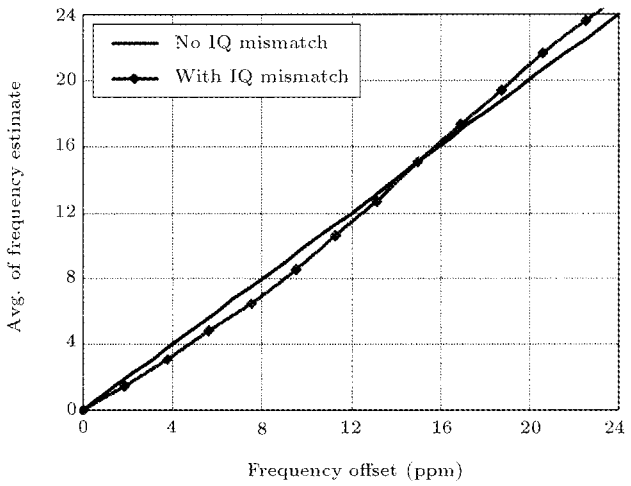

Figure 15. Average of the frequency offset estimate vs the true value.

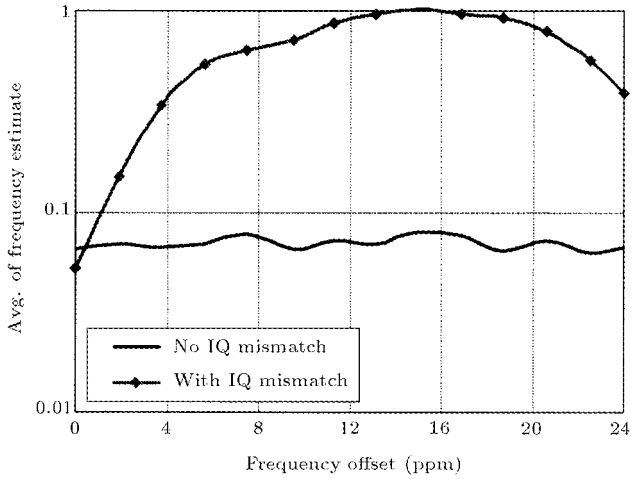

Figure 16. Standard deviation of the frequency offset estimate vs the true value.

offset, are no longer effective. To illustrate this point, Figure 15 also shows the average of the offset estimate when gain and phase mismatch values are set at 2 dB and 10 degrees, respectively. Clearly, the estimate obtained under these conditions is now biased, where the amount of bias changes with the value of the frequency offset.

In addition, Figure 16 also shows the standard deviation of the estimates obtained in the presence of IQ imbalance. It is observed that, in absence of IQ mismatch, the standard deviation of the estimate vs the actual frequency offset was relatively constant for the selected channel SNR with IQ imbalance present, the variance changes as frequency offset, are varied. Notice that even when the estimate has a small bias for certain values of frequency offset, the variance is relatively large. Such a poor performance was similarly observed when other frequency offset estimation algorithms were employed.

Similarly, while the IQ imbalance algorithms, described in the previous section, perform well for even large values of gain and estimation in the absence of frequency offset, they are not effective if frequency offset is non-zero, and the related phase rotation of the complex samples are not corrected. This is because Equations 5 and 6 are no longer valid in the presence of frequency offset. Indeed, if the samples exhibit small frequency offset or have not been corrected perfectly, the performances of the estimation algorithms are quite adversely affected. In this section, a new technique for frequency offset estimation is described, which is effective even in the presence of severe IQ mismatch [16-19]. Once the estimate is obtained, the complex samples can be corrected and, then, any effective technique for IQ imbalance estimation and compensation can be applied.

An equivalent model of the front-end of an OFDM receiver (with DC offsets and phase noise zero) is shown

in Figure 17, where the effects of the frequency offset and IQ imbalance are separated. It is straightforward to show (with some algebraic manipulations) that the two structures are identical.

Let one define $Y, \tilde{Y}$ and $\hat{Y}$, as the complex envelop of the desired received sequence (i.e., without the effect of frequency offset or IQ imbalance), the sequence after the inclusion of frequency offset effect and the sequence after further addition of IQ imbalance distortion, respectively.

Let one suppose that a specific OFDM symbol, $X_p[k]$, is formed such that only one of the sub-carriers, denoted by k_p, contains a non-zero value, i.e.,

$$X_p[k] = \begin{cases} P & \text{if} \quad k = k_p \\ 0 & \text{if} \quad k \neq k_p \end{cases},$$

where P denotes the symbol stored in sub-carrier k_p. When $X_p[k]$ is transmitted through the channel, using Equations 30 and 31, $\tilde{Y}[k]$, at sub-carrier k_p, becomes:

$$\tilde{Y}_p[k_p] = P \times H[k_p] \frac{\sin(\pi\beta)}{N \sin\left(\frac{\pi\beta}{N}\right)} e^{j\pi\beta\frac{N-1}{N}} + W[k_p], \tag{42}$$

where a subscript, p, is added to $\tilde{Y}[k]$ to indicate that this signal is due to symbol $X_p[k]$. At all other sub-carriers, one has:

$$\tilde{Y}_p[k] = P.H[k] \frac{\sin(\pi\beta)}{N \sin\left(\frac{\pi(k_p-k+\beta)}{N}\right)} e^{j\pi\beta\frac{N-1}{N}} . e^{j\pi\frac{k_p-k}{N}} + W[k], \qquad (k \neq k_p). \tag{43}$$

The above relation shows that, even in the absence of noise, all other sub-carriers (besides k_p) will contain non-zero terms, due to the ICI effects. These terms are, further, affected by IQ mismatch, according to Equation 7.

Notice that for a noiseless channel, if the frequency offset were zero, or if the samples were corrected

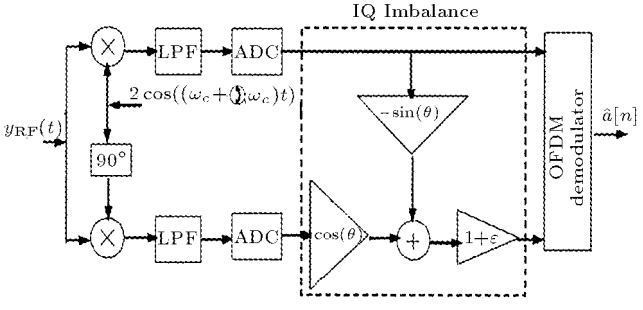

Figure 17. Model of a direct-conversion OFDM receiver with IQ imbalance and frequency offset.

for any non-zero offset, $\tilde{Y}_p[k]$ would only contain non-zero terms in sub-carrier k_p. With IQ imbalance, there would be non-zero terms at sub-carriers k_p and -k_p.

The basic principle behind the estimation algorithm is to find a value for the frequency offset estimate, such that the total power in all sub-carriers, except k_p and -k_p, is minimized. Toward that end, the following cost function is defined:

$$E_f = \sum_{\substack{k=-K \\ k\neq -k_p, k_p}} \left|\hat{Y}_p[k]\right|^2. \tag{44}$$

The algorithm, therefore, works as follows:

Step 1: Transmit a tone at the frequency $\omega_c + 2\pi k_p \Delta f$;

Step 2: Select an initial value for β;

Step 3: Correct the received samples for frequency offset, β;

Step 4: Compute E_f and choose a new estimate for β, with a reduced cost function, by moving in a direction opposite to the gradient of E_f, with respect to β;

Step 5: If the algorithm has not converged with sufficient desired accuracy, go to Step 3.

The algorithm above can be modified in a number of ways to allow for faster convergence. For example, the number of sub-channels in the transmitted OFDM symbol, $X_p[k]$, which contain non-zero terms, could be increased. This, in turn, will result in larger ICI terms when frequency offset is non-zero. In addition, in defining the cost function, a weight factor can be attributed to the magnitude for each sub-carrier, such that:

$$E_f = \sum_{\substack{k=-K \\ k\neq -k_p, k_p}}^{K} C[k] \left|\hat{Y}_p[k]\right|^2, \tag{45}$$

where $C[k]$ is a positive real term. The weight function above can be specified so that only sub-carriers which are closer to k_p and, hence, are expected to have more significant ICI values, would have larger values.

Figure 18 shows the average of the estimate of the frequency offset, using the above procedure vs the actual value, when the parameter β is changed from -0.15 to 0.15 (corresponding to -9.4 ppm to 9.4 ppm offset for an AWGN channel at a relatively high SNR). The plots show the results with and without IQ mismatch in the receiver mixer. With IQ imbalance present, the phase and gain imbalance parameters were, again, set at 10° and 2 dB, respectively. Here, to obtain the results, the transmit OFDM symbol was designed to contain two pilot tones. A weight function was designed so that the weight of the channel was lower

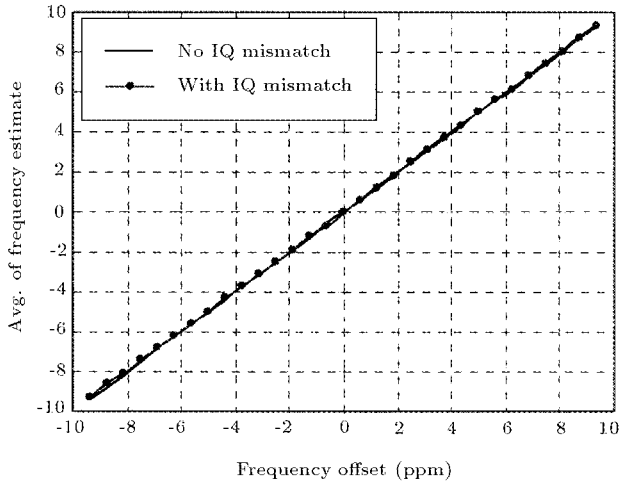

Figure 18. Average of the frequency offset estimate vs the true value.

the further it was from the pilots. Given the shape of the cost function, with a unique minimum in the range of interest, a variable step-size search mechanism was utilized. Here, if the value of E_f were higher for a new value of β, the step size would be lowered and β would be moved in a direction opposite to the previous change. On the other hand, if E_f were lower, the step size would remain the same and β would be moved in the same direction. This technique proved to result in fast convergence of the algorithm.

The plots show that the algorithm produces an unbiased estimate of the frequency offset in the presence and absence of IQ mismatch. The standard deviation of the estimate is also plotted in Figure 19, which shows that the variance does not vary as the frequency offset changes. As mentioned previously, once an estimate of the frequency offset is obtained and the samples are corrected, accordingly, an IQ imbalance compensation algorithm can be applied.

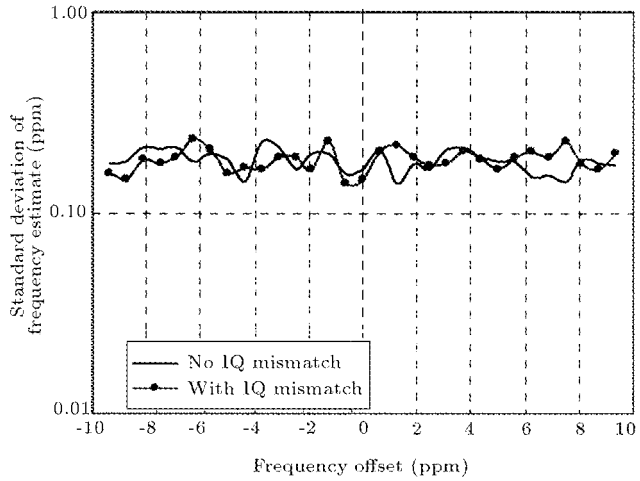

Figure 19. Standard deviation of the frequency offset estimate vs the true value.

PHASE NOISE

Noise and distortions at the output of the local oscillator could affect the performance of an OFDM system. Such effects include VCO phase noise, harmonics of the desired frequency or other unwanted frequency components. Of these, phase noise could hamper the bit-error-rate performance of the communication system quite adversely.

Phase noise is usually modeled by a Wiener process (sometimes referred to as Brownian motion), whose power spectral density is modeled by [19]:

$$S_\theta(f) = \frac{S_0}{1 + f^2/B^2}, \tag{46}$$

where B is the 3-dB bandwidth of the oscillator signal and S_0 is a constant. The phase noise spectrum, therefore, has a low-pass profile; a slope of -20 dB/decade, generally observed in typical oscillator implementations.

To investigate the effect of phase noise on an OFDM communication system, note that the received signal can be written as:

$$y(t) = x(t)e^{j\theta(t)}, \tag{47}$$

where, here, $\theta(t)$ is considered to be only due to phase jitter and not frequency offset. In the above relation, the channel is assumed to be ideal and the phase noise is considered to be the only distortion source. If the value of $\theta(t)$ is small, it can be approximated, using the following relation:

$$e^{j\theta(t)} \approx 1 + j\theta(t). \tag{48}$$

After sampling and OFDM demodulation, the sample at the kth sub-channel is given by:

$$\begin{aligned} Y(k) =& X(k) + jTX(k) \\ &+ \frac{j}{N}\sum_{l=-K}^{K}\sum_{n=0}^{N-1}\theta[n]X(k)e^{j2\pi\frac{l-k}{N}n}, \end{aligned} \tag{49}$$

where:

$$T = \frac{1}{N}\sum_{n=0}^{N-1}\theta[n]. \tag{50}$$

The above relation shows that phase noise affects the OFDM symbol in two ways. First, a phase term is added to all sub-carriers, which is observed as a rotation of the symbol constellation. The second effect is due to the third term on the RHD of Equation 49, which shows that phase noise disrupts the orthogonality between OFDM sub-carriers and results in inter-channel interference. The degradation in SNR,

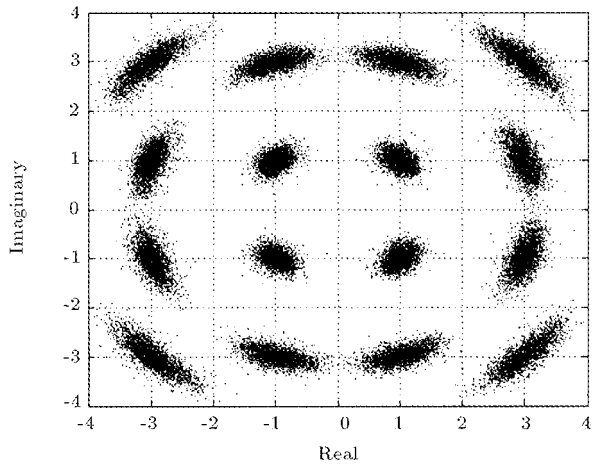

Figure 20. Effect of phase noise on the demodulated OFDM symbols (normalized bandwidth = 0.1).

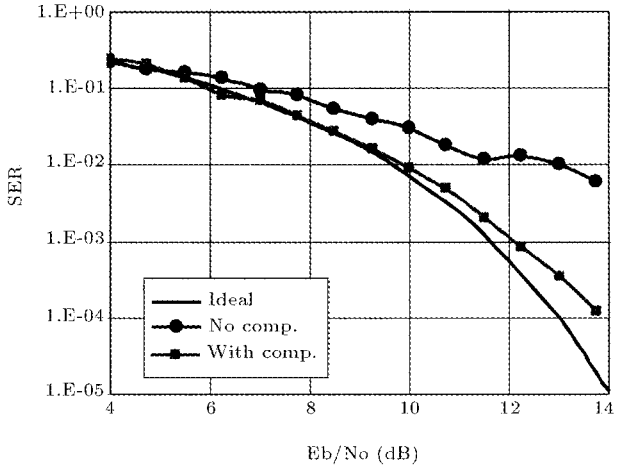

Figure 22. Effect of phase noise on the symbol error rate (normalized bandwidth = 0.1).

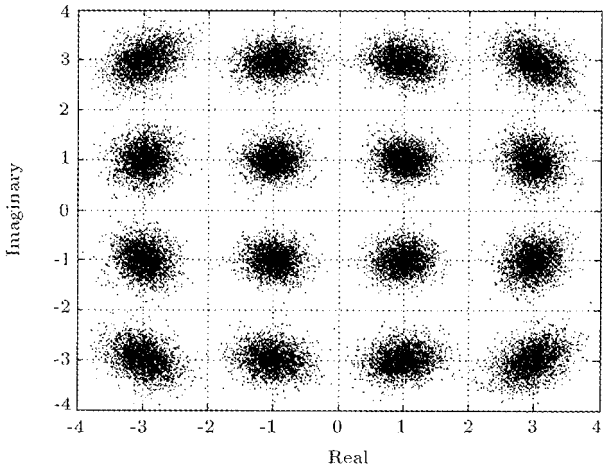

Figure 21. Effect of phase noise on the demodulated OFDM symbols (normalized bandwidth = 1).

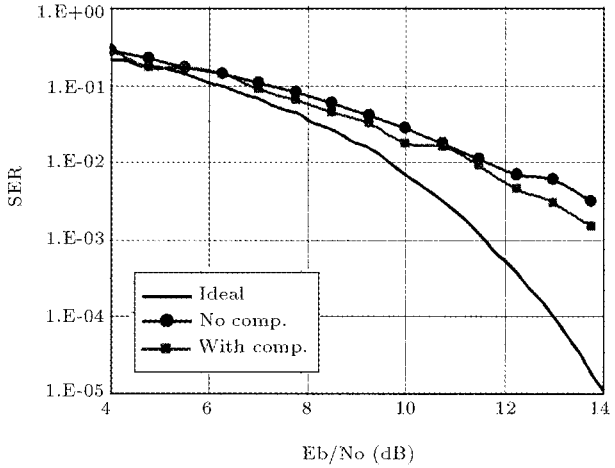

Figure 23. Effect of phase noise on the symbol error rate (normalized bandwidth = 1).

due to this term, clearly depends on the phase noise bandwidth. This distortion effect will be observed in the scattering of the symbols around their nominal positions in the constellation space.

To illustrate the above points, In Figures 20 and 21, symbol constellations, for an OFDM system with IEEE 802.11a parameters, are shown for two cases, where the normalized bandwidths, with respect to sub-carrier spacing, are 0.1 and 1, respectively. In both cases, noise power was set at 0.01. Notice that when the phase noise bandwidth is relatively small, symbols are rotated from their nominal positions.

As the bandwidth is increased (with the power kept fixed), the low-frequency contents contribute less and, hence, the amount of symbol rotation is decreased. More significantly, the ICI, due to high frequency components, causes the symbols to be dispersed around their ideal position. Figures 22 and 23 show the resulting degradation in the system symbol error rate for 16-QAM modulation, where about 2 orders of magnitude increase in SER is observed at SNR of 13 dB.

The effect of phase noise is clearly reduced by a careful design of radio components. In addition, the low-frequency content of the phase noise can be mitigated using the tracking algorithms for estimation and compensation of the frequency offset, as described in the previous section. Alternatively, the correction term can be incorporated into equalizer taps, if an adaptive equalizer, which would be designed to follow a slow variation of the fading channel, were utilized. In both cases, constant rotation of the constellation space is measured using pilot-sub-channels, or by monitoring the error between the received symbols and their corresponding detected symbols in a decision directed mode. Clearly, when the phase noise bandwidth is large and the amount of ICI is significant, the tracking or adaptation algorithms are no longer effective.

Figures 24 and 25 showed demodulated symbols when the tracking method described in the previous

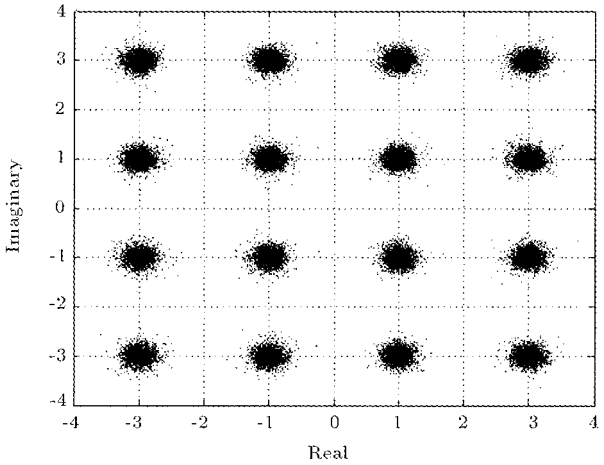

Figure 24. Effect of phase noise on the demodulated OFDM symbols (normalized bandwidth = 0.1).

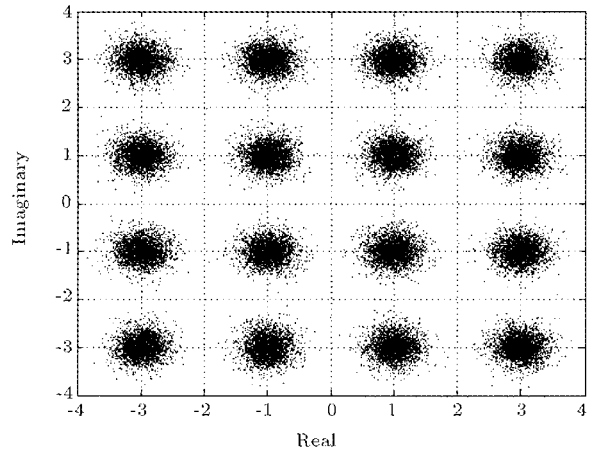

Figure 25. Effect of phase noise on the demodulated OFDM symbols (normalized bandwidth = 1).

section was in effect. It is observed in Figure 24 that when the noise bandwidth is low, the algorithm can adequately track phase variations and remove constellation rotation. On the other hand, in Figure 25, little improvement in signal constellation is observed since, as expected, ICI, due to high frequency phase noise, cannot be compensated by the tracking algorithm. Figures 22 and 23 show the related effect on the SER. While the SER has been substantially improved in the case of low-bandwidth (Figure 23), only a marginal improvement is observed when noise bandwidth is high.

CONCLUSIONS

In this paper, the effect of receiver non-idealities on the performance of an OFDM communication system was investigated. Specifically, issues related to IQ imbalance, frequency offset and phase noise effects were studied and methods for the compensation or mitigation of such effects were discussed. In each case, the proposed techniques were tested on an OFDM communication system design, based on the IEEE 802.11a specifications for wireless local area networks.

REFERENCES

1. Razavi, B. "Design consideration for direct conversion receivers", *IEEE Transaction on Circuits and Systems-II*, **3**(6), pp 344-352 (June 1997).
2. Mirabbasi, S. and Martin, K. "Classical and modern receiver architectures", *IEEE Comm. Magazine*, pp 132-139 (Nov. 2000).
3. Lassalle, R. and Alard, M. "Principles of modulation and coding for digital broadcasting of mobile receivers", *EBU Technical Review* (1992).
4. IEEE-SA Standards Board "Telecommunications and information exchange between systems-part 1", *High-Speed Physical Layer in the 5 GHz Band* (1999).
5. Nee, R.V. and Prasad, R., *OFDM for Wireless Multimedia Communications*, Artech House (2000).
6. Tubbax, J., Come, B., Van Der Perre, L., Deneire, L., Donnay, S. and Engels, M. "Compensation of IQ imbalance in OFDM systems", *IEEE International Conference on Communications*, **3**, pp 3403-3407 (May 2003).
7. Ylamurto, T.M. "Frequency domain IQ imbalance correction scheme for orthogonal frequency division multiplexing (OFDM) systems", *IEEE International Conference on Vehicular Technology*, **1**, pp 20-25 (Apr. 2003).
8. Fouladi Fard, S. and Shafiee, H. "Calibration of IQ imbalance in OFDM transceivers", *IEEE International Conference on Communications (ICC)*, **3**, pp 2071-2075 (May 2003).
9. Fouladi Fard, S. and Shafiee, H. "A new technique for estimation and compensation of IQ imbalance in OFDM receivers", *IEEE International Conference on Communication Systems (ICCS)*, Singapore, pp 223-227 (Nov. 2002).
10. Fouladi-Fard, S. and Shafiee, H. "Adaptive compensation of IQ imbalance in OFDM wireless communication systems", *Iranian Conference on Electrical Engineering (ICEE)*, Tabriz, Iran, pp 546-551 (May 2002).
11. Fouladi Fard, S. and Shafiee, H. "On adaptive compensation of IQ mismatch in OFDM receivers", *IEEE International Conference on Acoustics, Speech & Signal Processing (ICASSP)*, **4**, pp 564-567 (Apr. 2003).
12. Schuchert, A., Hasholzner, R. and Buchholz, M. "Frequency domain equalization of IQ imbalace in OFDM receivers", *IEEE International Conference on Consumer Electronics*, pp 28-29 (June 2001).
13. Moose, P.H. "A technique for orthogonal frequency division multiplexing frequency offset correction", *IEEE Transactions on Communications*, **42**, pp 2908-2914 (Oct. 1994).

14. Pollet, T., Van Blandel, M. and Moeneclaey, M. "BER sensitivity of OFDM systems to carrier frequency offset and wiener phase noise", *IEEE Transactions on Communications*, **43**(2/3/4), pp 191-193 (Feb./March/Apr. 1995).

15. Classen, F. and Meyr, H. "Frequency synchronization algorithms for OFDM systems suitable for communication over frequency selective channels", *Proc. VTC*, Stockholm, Sweden, pp 1655-1659 (June 1994).

16. Shafiee, H. "Frequency offset estimation in OFDM systems in presence of IQ imbalance", *IEEE International Conference on Communication Systems*, Singapore, pp 213-217 (Nov. 2002).

17. Fouladi Fard, S. and Shafiee, h. "An effective method for the estimation of frequency offset in wireless OFDM systems with IQ imbalance", *IEEE International Conference on Communications (ICC)*, **3**, pp 2081-2085 (May 2003).

18. Fouladi Fard, S. "Analysis and compensation of IQ imbalance effects in wireless OFDM syetems", MSc. Thesis, University of Tehran, Tehran, Iran (June 2003).

19. Armada, A.G. "Understanding the effect of phase noise in orthogonal frequency division multiplexing (OFDM)", *IEEE Transactions on Broadcasting*, **47**(2) (June 2001).